

## Enhanced backward emission of heavy fragments in high-energy proton-nucleus collisions

J. Hüfner

*Institut für Theoretische Physik der Universität Heidelberg,  
6900 Heidelberg, Federal Republic of Germany*

H. M. Sommermann

*Max-Planck-Institut für Kernphysik, 6900 Heidelberg, Federal Republic of Germany  
(Received 28 December 1982)*

The conventional description of high energy proton-nucleus collisions in terms of an intranuclear cascade and compound nuclear decay (the two-step model) breaks down at projectile energies  $E_p > 10$  GeV. Unusual backward enhancements are found in the angular distribution of heavy fragments (Sc, Cu) from uranium targets. This effect is explained in a fast breakup model of deep spallation/cleavage processes. The observed backward emission originates in the competition between (backward-directed) Coulomb repulsion and (forward-directed) momentum components from recoiling nucleons.

NUCLEAR REACTIONS  $^{238}\text{U}(p,x)^{47}\text{Sc}$ ;  $T_p=40\text{--}400$  GeV, cleavage  
model to explain double differential cross section.

## I. CLEAVAGE OR FAST BREAKUP OF NUCLEI

This is the conventional picture of high-energy proton-nucleus collisions, as proposed by Serber<sup>1</sup>: In the first step of the reaction the projectile interacts with the individual constituents of the target and an intranuclear cascade develops. Several nucleons and light clusters are promptly ejected. The resulting nucleus is highly excited and moves forward. In the second step of the reaction, assumed to take place on a slower time scale, the excitation energy is dissipated by the evaporation of nucleons and light nuclei and possibly by fission. From this picture of the proton-nucleus reaction the following properties of the angular distribution are deduced immediately: There must exist a forward moving frame in which the observed evaporated nucleons and fragments are emitted isotropically (or at least symmetrically around  $90^\circ$ ). If transformed to the laboratory system, more particles are expected at forward than at backward angles. These predictions have been verified in many cases and the two-step model has generally been accepted as correctly describing the underlying physics.

In recent years, however, several experiments, e.g., those by Wilkins *et al.*,<sup>2</sup> have produced results which cannot be explained by the conventional model. The most clear-cut evidence against the two-step model are angular distributions which show in the laboratory system that more particles are emitted under backward than at forward angles

(Fig. 1). These unusual backward enhancements have been observed in proton-uranium reactions at energies above 10 GeV, for heavy fragments like  $^{47}\text{Sc}$  and  $^{64}\text{Cu}$ , by Porile *et al.*<sup>4</sup> and Fortney *et al.*<sup>5</sup> Fragments in the mass range  $30 < A < 70$ , which is far removed from the target mass ( $^{238}\text{U}$ ), cannot represent the evaporation residues of symmetric fission, nor can they result from the statistical evaporation of a compound system. Nuclei in this mass region are often said to be formed in a "deep spallation" process, a notion which has never received a proper definition in terms of a physical process.

Recently, Fortney *et al.*<sup>3</sup> measured not only the angular distribution  $d\sigma/d\Omega$  of emitted fragments ( $^{47}\text{Sc}$ ) but, in addition, the double differential cross section  $d^2\sigma/d\Omega dE$ , where  $E$  denotes the kinetic energy of the fragment. For energies  $E$  below the barrier (defined as the peak of the energy distribution) a strong backward enhancement is found, while the angular distribution is forward peaked for large energies  $E$  of the emitted fragment (Fig. 1). This effect inspired us to propose an explanation of the experimental data which is based on a fast breakup or cleavage mechanism for the production of heavy fragments. Bohrmann *et al.*<sup>6</sup> have employed this model for the calculation of the mass yield curve and energy distributions in the deep spallation domain. This model also provides, to our knowledge, the first explanation of the enhanced backward emission of heavy fragments and observed variation with energy of the angular distribution, as

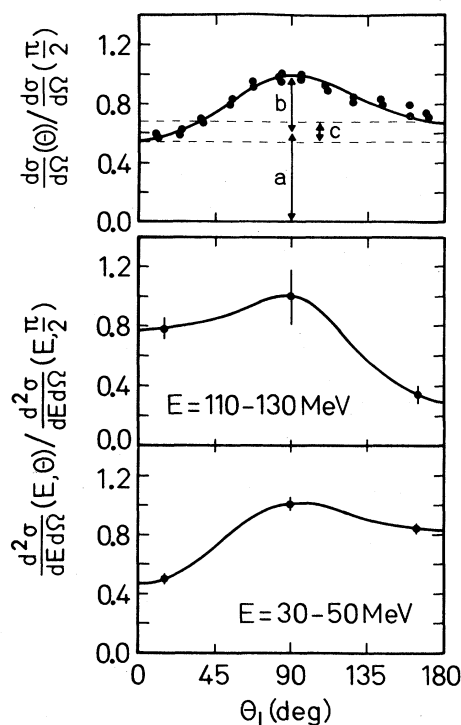


FIG. 1. Unusual backward enhancement in the angular distribution (laboratory system) of  $^{47}\text{Sc}$  fragments from the reaction  $p + ^{238}\text{U} \rightarrow ^{47}\text{Sc} + X$  ( $E_p = 400$  GeV). The differential cross section  $d\sigma/d\Omega$  (upper part) contains a dominant isotropic component (a) and substantial side-ward peaking (b); in addition a small backward enhancement (c) is observed. The origins of the individual contributions (a)–(c) are discussed in connection with our model in Sec. II. The double differential cross section  $d^2\sigma/dE d\Omega$  is shown in the lower parts: High-energy fragments ( $E = 110\text{--}130$  MeV) are forward peaked, while fragments with small kinetic energies ( $E = 30\text{--}50$  MeV) are predominantly emitted in the backward direction. The results displayed in this figure have been taken from Ref. 3.

will be shown in the present paper.

A schematic picture of the cleavage process, as envisaged by us, is given in Fig. 2: The highly energetic proton projectile ( $E_p = 40\text{--}400$  GeV) drills a trumpet-shaped hole into the target nucleus. Several nucleons, which are hit by the projectile along its way, are propelled into the sides of this hole. These spray particles transfer energy and momentum to the surrounding matter and cause an instability which propagates and, eventually, leads to the disintegration of the system. In this way, the hole does not “heal,” but continues to grow, provided that the breaking point of nuclear matter (Bertsch *et al.*<sup>7</sup>) can be overcome. In the most probable case (the statistical distribution of impact parameters) one heavy and one light prefragment are formed. This predic-

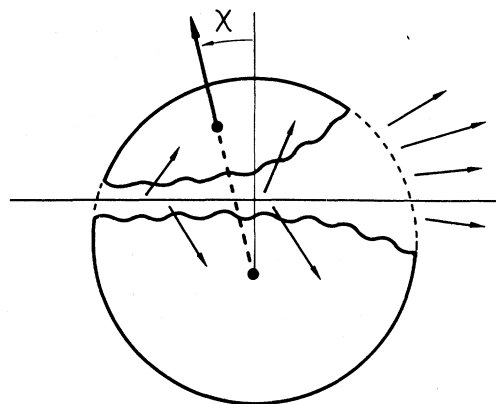


FIG. 2. Fast breakup model of cleavage/deep spallation reactions. The highly energetic incident projectile creates a trumpet shaped channel in the target nucleus. Several nucleons and light nuclei are promptly ejected (forward arrows); a number of nucleons are propelled sideways (inside arrows) creating an instability which leads to the disintegration of the system. The resulting (pre)fragments receive momentum contributions from the Fermi motion of nucleons, the recoiling secondary nucleons (arrows), the Coulomb repulsion (under direction  $\chi$ ), and statistical evaporation. The Coulomb repulsion leads to the unusual backward enhancement in the angular distribution of (the smaller) reaction fragments (see the discussion in Sec. II).

tion is consistent with the observed correlation between fragment masses (Wilkins *et al.*<sup>2</sup>). It is plausible, furthermore, that due to its larger curvature at the “front edge” of the lighter fragment breaks off. Its center of mass is therefore displaced with respect to that of the heavier fragment (by an angle  $\chi$ , Fig. 2) into the backward direction.

The similarities and the differences between the cleavage process, described here, and the conventional two-step model are the following: In both cases a fast intranuclear cascade is initiated by the projectile proton and results in a highly unstable target nucleus: In the conventional model all instabilities “heal out,” leading to the thermalization of the system. The energy of the hot nucleus is dissipated via evaporation. In the cleavage model the primary instabilities *do not* heal but expand, causing a breakup of the target nucleus. The corresponding prefragments may be excited and evaporate nucleons.

The purpose of this paper is to develop a model describing cleavage or fast breakup reactions. The consistency of the predictions of our model with the experimental data and, in particular, the occurrence of backward enhancements in the angular distribution of heavy fragments, serve to establish the existence and to clarify the mechanism of the cleavage process. This work is largely phenomenological.

We present in this paper an analysis for the double differential cross section  $d^2\sigma/d\Omega dE$  in the reaction



at proton energies between 40 to 400 GeV.

## II. THE DOUBLE DIFFERENTIAL CROSS SECTIONS

The highly energetic proton projectile has drilled a hole through the target nucleus (Fig. 2); the target has broken up into two prefragments, and several fast nucleons and pions. We concentrate now on the smaller prefragment (Fig. 2) which eventually evaporates nucleons to become the observed fragment. The momentum distribution of the prefragment is determined by three sources:

(i) An isotropic contribution from the *Fermi motion* of nucleons. If a nucleus is cut into two or more pieces in a rapid way, such that the nucleons in each piece keep their Fermi momentum, each prefragment is left with a momentum  $\vec{k}$  whose mean square value is

$$\sigma_F^2 = \frac{1}{3} \langle \vec{k}^2 \rangle = \frac{k_F^2}{5} A_{\text{PF}} \frac{A_T - A_{\text{PF}}}{A_T - 1}; \quad (2)$$

an expression first given by Goldhaber.<sup>8</sup>  $k_F$  denotes the Fermi momentum;  $A_{\text{PF}}$  and  $A_T$  represent the nucleon numbers of the prefragment and target, respectively.

(ii) The sideward-to-forward directed momentum  $\vec{q}$  from the *spray particles*, which are ploughed out of the hole by the projectile and deposit energy and momentum in the prefragment. The momentum transfer in high energy  $p$ - $p$  collisions possesses a transverse component whose mean value is  $\langle q_{\perp}^2 \rangle_{NN}^{1/2} \simeq 0.3$  GeV/ $c$  universally. The longitudinal component for elastic scattering assumes a value

$$\langle q_{\parallel} \rangle_{NN} \simeq \langle q_{\perp}^2 \rangle_{NN} / 2m_p c \simeq 50 \text{ MeV}/c$$

and increases substantially with the inelasticity of the reaction. In each case  $q_{\parallel} > 0$  and, hence,  $\vec{q}$  contributes to the forward motion of the fragments.

(iii) The sideward-to-backward directed momentum from *Coulomb repulsion*. After cleavage the fragments are separated, i.e., outside the range of their mutual nuclear attraction. But they are subject to the Coulomb force. In the geometry shown in Fig. 2, this force has a backward directed component proportional to  $\sin\chi$  and a transverse component proportional to  $\cos\chi$ .

The moving prefragment evaporates nucleons. We have estimated that this process does not significant-

ly change the angular distribution. It was, therefore, neglected in the present treatment.

The individual contributions to the total momentum distribution described above can be recognized in the differential cross section  $d\sigma/d\Omega$  given in Fig. 1 (upper part). We identify the large isotropic part of the cross section [denoted by (a) in Fig. 1] with the contribution from the Fermi motion of nucleons. The enhancement of  $d\sigma/d\Omega$  at  $90^\circ$  over the average of the cross sections at  $0^\circ$  and  $180^\circ$  [denoted by (b)] is caused by the transverse momentum components of the spray particles and the Coulomb force. The forward/backward asymmetry [denoted by (c)] arises from the competition between the backward-directed push of the Coulomb force and the forward-directed kicks from spray particles.

The momentum distribution of the observed fragments is obtained, according to the above arguments, as

$$\frac{d^3\sigma}{dp^3} = B_0 \int \int \int d^3k d^3q d^3t F_F(\vec{k}) F_S(\vec{q}) \times F_C(\vec{t}; \vec{k}, \vec{q}) \delta(\vec{p} - \vec{k} - \vec{q} - \vec{t}). \quad (3)$$

Here,  $B_0$  contains the normalization factors. The distribution functions  $F$  describe the effects of Fermi motion ( $F_F$ ), of spray particles ( $F_S$ ), and of the Coulomb repulsion ( $F_C$ ). We assume a Gaussian for

$$F_F(\vec{k}) = e^{-k^2/2\sigma_F^2}, \quad (4)$$

where  $\sigma_F$  is given by Eq. (2). For the momentum distribution from spray particles we write

$$F_S(\vec{q}) = e^{-q_{\perp}^2/2\sigma_q^2} \delta(q_{\parallel} - \bar{q}_{\parallel}), \quad (5)$$

with two parameters  $\sigma_q^2$  and  $\bar{q}_{\parallel}$ , where the component  $\bar{q}_{\parallel}$  must always be positive. Since only the order of magnitude of  $\bar{q}_{\parallel}$  and  $\sigma_q^2$  are known, their precise values have to come from a fit of the theoretical distribution to the experimental data. We estimate

$$\bar{q}_{\parallel} \simeq \nu \langle q_{\parallel} \rangle_{NN}, \quad \sigma_q^2 \simeq \nu \frac{1}{2} \langle q_{\perp}^2 \rangle_{NN}, \quad (6)$$

where  $\nu$  is the number of spray particles which are stopped in the prefragment. While  $\langle q_{\perp}^2 \rangle_{NN}^{1/2} \simeq 300$  MeV/ $c$  universally, the value of  $\langle q_{\parallel} \rangle_{NN}$  is not known precisely. From the kinematics of elastic scattering we deduced a lower limit  $\langle q_{\parallel} \rangle_{NN} \geq 50$  MeV/ $c$ . An upper limit can be obtained from the requirement that those spray particles which enter the prefragment move at least under  $45^\circ$  with respect to the beam axis; therefore

$$\langle q_{\parallel} \rangle_{NN} \lesssim (\langle q_{\perp}^2 \rangle_{NN}/2)^{1/2} \simeq 200 \text{ MeV}/c .$$

Although the motion of the lighter prefragment in the Coulomb field of the heavy partner can be calculated exactly, there exists no simple analytic expression. Furthermore, the complicated, and at present unknown, shape of the geometrical configuration at the moment of cleavage makes any detailed calculation questionable. The Coulomb interaction was treated, therefore, in a "minimal theory" based on energy conservation

$$\vec{p}^2 = (\vec{k} + \vec{q} + \vec{t}_C)^2 = 2M_R V_C + (\vec{k} + \vec{q})^2, \quad (7)$$

where  $M_R$  is the reduced mass of the prefragment.  $V_C$  denotes the Coulomb barrier at the point of cleavage; its magnitude may be estimated from the peak in the experimental energy distribution  $d\sigma/dE$ . The longitudinal and transverse components of  $\vec{t}$ , the momentum of the fragment due to Coulomb

repulsion, are given by  $t_{\parallel} = -t_C \sin\chi$  and  $|t_{\perp}| = t_C \cos\chi$ , respectively (Fig. 2). From Eq. (7) one obtains the approximate expression

$$t_C \simeq M_R V_C / |\vec{p}| . \quad (8)$$

The distribution  $F_C$  can then be written as

$$F_C(\vec{t}, \vec{p}) = \Theta(p^2 - 2M_R V_C) \delta(\vec{t} - \vec{t}_C), \quad (9)$$

with the classical barrier function  $\Theta(p^2 - 2M_R V_C)$ . This  $\Theta$  function should be modified due to tunneling. According to Eq. (8) the Coulomb push,  $t_C$ , is inversely proportional to the fragment momentum  $|\vec{p}|$ : The influence of the Coulomb force is largest for small observed fragment energies, and therefore backward peaking is most pronounced for small  $E$  [confer Fig. 1 (lower part)].

With the assumption  $\sigma_q^2/\sigma_F^2 \ll 1$  and  $t_C^2/\sigma_F^2 \ll 1$ , the integral Eq. (3) can be evaluated and we obtain

$$\frac{d^3\sigma}{dp^3}(p, \theta) = B_1(|\vec{p}|) e^{-p^2/2\sigma_F^2} \left\{ 1 + \frac{(2\sigma_F)^2 p (\bar{q}_{\parallel} - t_C \sin\chi)}{(2\sigma_F^2)^2 + p^2(2\sigma_q^2 + t_C^2 \cos^2\chi)} \cos\theta - \frac{p^2(2\sigma_q^2 + t_C^2 \cos^2\chi)}{(2\sigma_F^2)^2 + p^2(2\sigma_q^2 + t_C^2 \cos^2\chi)} \cos^2\theta \right\}, \quad (10)$$

where  $\theta$  is the angle, in the laboratory system, between the fragment momentum  $\vec{p}$  and the beam axis.  $B_1(|\vec{p}|)$  is proportional to the barrier penetration function. By converting momenta into energies ( $E = p^2/2M$ ) and introducing the energy dependence of  $t_C$  via Eq. (8), the double differential cross section can be cast into the form

$$\frac{d^2\sigma}{d\Omega dE} = B(E) e^{-E/E_0} \left\{ 1 + \frac{a\sqrt{E} - b}{d + E} \cos\theta - \frac{c + E}{d + E} \cos^2\theta \right\}. \quad (11)$$

The explicit expression for the constants  $a$ ,  $b$ ,  $c$ , and  $d$  can be obtained from the comparison of Eqs. (10) and (11). With the above definitions all constants  $a$  through  $d$  are positive. The exponential contains  $E_0 = \sigma_F^2/M$ . Note that

$$E_0 \simeq \frac{1}{3} k_F^2 / 2m_p = \frac{1}{3} \epsilon_F$$

with the Fermi energy  $\epsilon_F \simeq 40$  MeV. This explains the observed exponential decrease of the energy distribution (Fortney *et al.*<sup>3</sup>) with a universal constant  $E_0 \simeq 15$  MeV (Bohrmann *et al.*<sup>6</sup>).

The experimental angular distribution of Fortney *et al.*<sup>3</sup> is given in the form

$$F(E, \theta) = \frac{d^2\sigma(E, \theta)/d\Omega dE}{d^2\sigma(E, \pi/2)/d\Omega dE} = \{1 + A_1(E) \cos\theta + A_2(E) \cos^2\theta\}. \quad (12)$$

Furthermore, the quotient  $F/B$  is defined as the ratio of forward to backward emission,

$$\frac{F}{B}(E) = \int_0^{\pi/2} d(\cos\theta) F(E, \theta) / \int_{\pi/2}^{\pi} d(\cos\theta) F(E, \theta). \quad (13)$$

The experimental values of the coefficients  $A_1(E)$ ,  $A_2(E)$ , and  $(F/B)(E)$  are shown by solid dots in Fig. 3. Their theoretical expressions can be read from Eq. (11).

Experimentally  $A_2(E)$ , which is related to side-

ward peaking, is always negative.  $A_1(E)$ , which determines the forward/backward ratio, is negative for small energies (implying backward enhancement), and changes sign around the barrier (causing forward enhancement). The position of the barrier

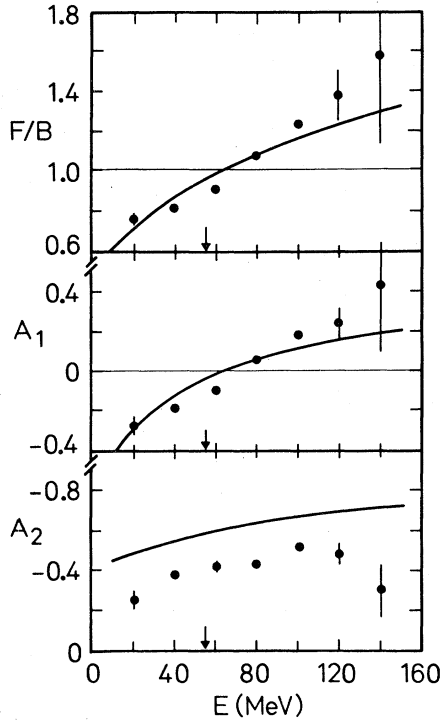


FIG. 3. Energy dependence of the forward/backward ratio  $F/B$  and coefficients  $A_1(E)$ ,  $A_2(E)$  of the angular distribution

$$d^2\sigma/d\Omega dE \propto (1 + A_1(E)\cos\theta + A_2(E)\cos^2\theta).$$

The solid dots represent the experimental data of Fortney *et al.*<sup>3</sup> for the reaction  $p + {}^{238}\text{U} \rightarrow {}^{47}\text{Sc} + X$  at  $E_p = 400$  GeV. The solid curves are calculated within the cleavage model.

is indicated by the arrow in Fig. 3. It is clear that our model will predict the correct sign of  $A_2(E)$ , since the coefficients  $c$  and  $d$  of Eq. (11) are positive. Similarly, the qualitative behavior of  $A_1(E)$  is contained in the theoretical expression

$$A_1(E) = (a\sqrt{E} - b)/(d + E).$$

$A_1(E)$  is negative for small energies and positive for large values of  $E$ ; however, the linear dependence on the energy  $E$ , which is suggested by the experimental data, is not reproduced. The reason for this apparent discrepancy may lie in the approximations which lead to Eq. (9).

In order to determine the constants  $a$  through  $d$ , and from them the constants  $\sigma_F$ ,  $\sigma_q$ ,  $\bar{q}_{||}$ ,  $\chi$ , and  $V_C$ , we have fit the double differential cross section Eq. (11) to the experimental data (Fig. 3). We have not attempted a best fit, but rather "reasonable" agreement, i.e., a compromise between the most accurate description of the data and a choice of parameters which is in line with our expectations. Our results

for  $A_1(E)$  and  $A_2(E)$  are shown in Fig. 3. The obtained constant  $\sigma_F$ , which characterizes the Fermi motion, is  $\sigma_F = 800$  MeV/ $c$  for a  ${}^{238}\text{U}$  target and  ${}^{47}\text{Sc}$  fragment (prefragment mass  $A_{PF} \approx 65$ ). This value of  $\sigma_F$  is somewhat larger than the one given by Eq. (2) and more in line with the constant  $E_0$  of the exponential decay of the energy distribution Eq. (11). The inelastically scattered secondary nucleons are characterized by the constants  $\sigma_q \approx 350$  MeV/ $c$  and  $\bar{q}_{||} \approx 350$  MeV/ $c$ . These values are compatible with a number  $\nu \sim 2$  of spray particles which enter into the prefragment and are stopped [see Eq. (6)]. The same order of magnitude for the longitudinal momentum transfer is observed in proton or light ion reactions on U which lead to fission (Saint Laurent *et al.*<sup>9</sup>). The angle  $\chi$  under which the repulsive Coulomb force acts on the escaping prefragment has been chosen as  $\chi = 38^\circ$ , a value which appears on the limit of the acceptable range. The magnitude of the Coulomb barrier  $V_C \approx 35$  MeV, deduced from the angular distribution, is of the order of the energy which corresponds to the maximum in the energy distribution (Fortney *et al.*<sup>3</sup>). Thus we have indeed found a reasonable fit with reasonable parameters, in support of the physical assumptions of the cleavage model.

### III. CONCLUSIONS

The investigation of the mechanism of cleavage or deep spallation processes is still in the exploratory stage. Therefore any success of an *ad hoc* model like ours should be met with criticism. Cleavage is a fast breakup of a nucleus into two or more heavy fragments caused by bombardment with high-energy projectiles. We do not know how the fragment breaks around the instability created by the projectile. Nevertheless, from the geometry of the process the absolute cross section for the observed fragments can be predicted without any free parameter and agrees with experiment (Bohrmann *et al.*<sup>6</sup>). In this paper we have studied the momentum distribution or the double differential cross section  $d^2\sigma/d\Omega dE$ . The Fermi momentum dominates, Coulomb repulsion and momentum contributions from knocked-on nucleons add up in the transverse direction; their longitudinal components, however, have opposing effects. The trumpet shaped geometry (Fig. 2), which is essential in order to have a backward directed Coulomb force, appears to be the weakest point of our model. It was necessary, furthermore, to fit several parameters. The obtained values are reasonable and correspond to our expectations within a factor of 2 or better. The predictions of the present cleavage model are consistent with the experimental data.

Barium isotopes are probable partners for scandium fragments in high-energy proton-uranium cleavage reactions. If the angular distribution for Sc is backward peaked, the distribution of the Ba partner should have the opposite behavior. Porile *et al.*<sup>4</sup> have measured the differential cross section  $d\sigma/d\Omega$  for <sup>128</sup>Ba and <sup>140</sup>Ba and, indeed, find dominant forward emission in both cases.

In the same experiment Porile *et al.*<sup>4</sup> also report a slight forward peaking for Mg fragments. What is the origin of this result? In our treatment, the forward-peaked asymmetry represents a balance between two effects: the backward directed Coulomb force and the push of spray particles in the forward direction. These two opposing effects can be clearly seen in the energy dependence of  $A_1(E)$  (Fig. 3). After integration over energy, only a small net effect remains, which is sensitive to the location of the maximum in the energy distribution, among other details. For instance, a reduction of the Coulomb barrier (in the case of Mg) may weaken the influence of the backward directed Coulomb force and thus lead to an overall forward peaking.

The target mass ( $A_T$ ) dependence of the differential cross section  $d\sigma/d\Omega$  for <sup>47</sup>Sc fragments, produced in the reaction  $p + A_T \rightarrow ^{47}\text{Sc} + X$  ( $E_p = 400$  GeV), has been investigated by Stewart *et al.*<sup>10</sup> Unfortunately, no double differential cross sections have been measured. In the case of heavy targets (Lu, Au, U) strong sideward peaking in  $d\sigma/d\Omega$  is observed. In addition, a backward enhancement is visible for the heaviest nuclei (Au,

U). For lighter targets (Ag, La) the angular distribution is peaked in the forward direction. The preferred backward emission of Sc fragments hence is restricted to reactions with heavy targets. This effect may be understood in terms of our model. When bombarding <sup>238</sup>U nuclei, the detected <sup>47</sup>Sc fragments are expected to be the evaporation residues of the *lighter* prefragments which, due to the Coulomb repulsion, are preferably emitted backward. For <sup>139</sup>La and <sup>107</sup>Ag targets the situation is reversed: <sup>47</sup>Sc fragments now come most likely from the *heavier* prefragments whose angular distribution, according to our model, is *always* forward peaked (Fig. 2). However, we cannot exclude the possibility that the latter Sc fragments are produced in the conventional two-step process of excitation and evaporation. Further experimental measurements, especially of the double differential cross section  $d^2\sigma/dE d\Omega$  and angular correlations for light and heavy fragments, are necessary to distinguish between the two processes and to gain further insight into the detailed mechanism and the dynamics of deep spallation or cleavage reactions.

#### ACKNOWLEDGMENTS

We thank S. Bohrmann and E. P. Steinberg for discussions. Correspondence with B. D. Wilkins is gratefully acknowledged. This work was supported in part by the Federal Ministry for Research and Technology (BMFT).

<sup>1</sup>R. Serber, Phys. Rev. **72**, 1114 (1947).

<sup>2</sup>B. D. Wilkins, S. B. Kaufman, E. P. Steinberg, J. A. Urbon, and D. J. Henderson, Phys. Rev. Lett. **43**, 1080 (1979).

<sup>3</sup>D. R. Fortney and N. T. Porile, Phys. Rev. C **22**, 670 (1980).

<sup>4</sup>N. T. Porile *et al.*, Phys. Rev. Lett. **43**, 918 (1979).

<sup>5</sup>D. R. Fortney and N. T. Porile, Phys. Rev. C **21**, 2511 (1980).

<sup>6</sup>S. Bohrmann, J. Hüfner, and M. C. Nemes, Phys. Lett. **120B**, 59 (1983).

<sup>7</sup>G. F. Bertsch and D. Munding, Phys. Rev. C **17**, 1646 (1978).

<sup>8</sup>A. S. Goldhaber, Phys. Lett. **53B**, 306 (1974).

<sup>9</sup>F. Saint Laurent *et al.*, Phys. Lett. **110B**, 372 (1982).

<sup>10</sup>J. S. Stewart and N. T. Porile, Phys. Rev. C **25**, 478 (1982).